ACS OMEGA

http://pubs.acs.org/journal/acsodf

Article

Anisotropic Impact Sensitivity of Metal-Free Molecular Perovskite High-Energetic Material $(C_6H_{14}N_2)(NH_2NH_3)(ClO_4)_3$ by First-Principles Study

Qiaoli Li, Shenshen Li, Minghe Qu, and Jijun Xiao*

Cite This: *ACS Omega* 2022, 7, 17185−17191

Read Online

ACCESS | Metrics & More | Article Recommendations

ABSTRACT: Density functional theory simulations were carried out to investigate energetic molecular perovskite $(C_6H_{14}N_2)(NH_2NH_3)(ClO_4)_3$ which was a new type energetic material promising for future application. The electronic properties, surface energy, and hydrogen bonding of (100), (010), (011), (101), (111) surfaces were studied, and the anisotropic impact sensitivity of these surfaces were reported. By comparing the values of the band gaps for different surface structures, we found that the (100) surface has the lowest sensitivity, while the (101) surface was considered to be much more sensitive than the others. The results for the total density of states further validated the previous conclusion obtained from the band gap. Additionally, the calculated surface energy indicated that surface energy was positively correlated with impact sensitivity. Hydrogen bond content of the surface structures showed distinct variability according to the two-dimensional fingerprint plots. In particular, the hydrogen bond content of (100) surface was higher than that of other surfaces, indicating that the impact sensitivity of (100) surface is the lowest.

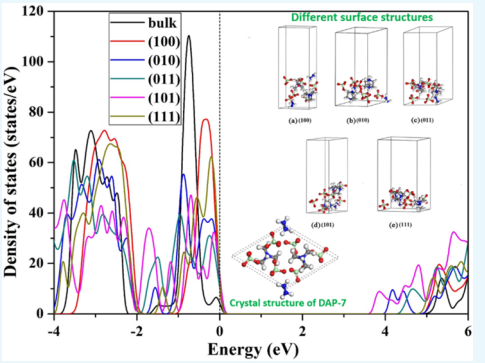

1. INTRODUCTION

Energetic materials are a class of special reactive substances storing large amounts of chemical energy, including explosives, propellants, and pyrotechnics.[1,2] With the rapid development of modern military science and technology and aerospace industry, the requirements for energetic materials are also increasing. In order to adapt to a harsher environment and cope with various extreme conditions in the universe, the new generation of energetic materials must have good comprehensive performance including high energy, low sensitivity, low cost, and functional diversity.[3] Driven by both synthetic and theoretical research, new structures of energetic materials are emerging.[4,5] However, the high detonation performance and low sensitivity are mutually exclusive for most of explosives. Few explosives could meet the practical applications of weapons and equipment effectively. Therefore, designing new structures and exploring new concepts of energetic compounds are still the main research hotspots in the field of energetic materials.[6,7]

In recent years, molecular perovskites have played an important role in many areas, including solar cells,[8−10] thermoelectricity,[11] ferroelectrics,[12] piezoelectricity,[13] lasers,[14] and so on due to their unique structures and excellent properties.[15] Lately, Chen's team[16−18] has designed and synthesized a series of high-energy-density compounds with molecular perovskite structure characteristics, which created a precedent for molecular perovskite in the field of energetic materials. Different from traditional energetic compounds, these energetic molecular perovskites are composed of special oxidative ions (like ClO_4^-) and organic cations (as fuel part). Most importantly, these energetic molecular perovskites have the advantages of excellent detonation performances, good stability, and low cost. The emergence of molecular perovskites high-energetic materials is undoubtedly of great significance to the development of energetic materials. Among them, the metal-free molecular perovskite $(H_2dabco)(NH_4)(ClO_4)_3]$ (DAP-4 for short) has attracted great attention to researchers because of the high exothermic effect and high amount of gas.[19−24] Compared to DAP-4, the metal-free molecular perovskite $(H_2dabco)(NH_2NH_3)(ClO_4)_3$ (DAP-7 for short)[18] not only possesses more excellent detonation performances and better thermal stability but has great potential to be used as a heat-resistant explosive.

Sensitivity is an important index to measure the stability of explosives, which is usually defined as the degree of difficulty of decomposition or explosion for energetic materials under external stimulation (impact, friction, etc.).[25] According to

Received: February 13, 2022
Accepted: April 19, 2022
Published: May 10, 2022

https://doi.org/10.1021/acsomega.2c00878
ACS Omega 2022, 7, 17185−17191

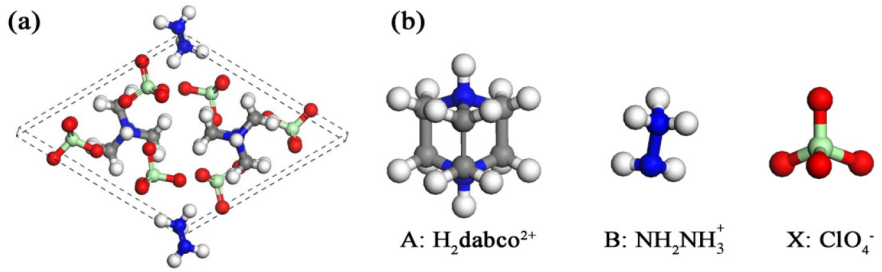

Figure 1. (a) Crystal structure of DAP-7. (b) Ion composition. H atom in light gray, C atom in dark gray, N atom in blue, O atom in red, and Cl atom in green.

Table 1. Experimental and Calculated Lattice Parameters of DAP-7

methods	*a* (Å)	*b* (Å)	*c* (Å)	*B* (deg)	volume (Å^3)
experiment[18]	10.378	8.050	10.587	117.99	781.034
PBE	10.783	8.042	11.0766	119.16	838.794
	(+3.90%)	(−0.10%)	(+4.63%)	(+0.98%)	(+7.39%)
PBE+D3	10.353	7.945	10.608	118.66	765.622
	(−0.24%)	(−1.31%)	(+0.20%)	(+0.56%)	(−1.97%)
PBEsol	10.486	7.839	10.753	119.00	773.057
	(+1.04%)	(−2.62%)	(+1.57%)	(+0.85%)	(−1.02%)
PBEsol+D3	10.191	7.799	10.432	118.62	727.850
	(−1.80%)	(−3.12%)	(−1.46%)	(+0.53%)	(−6.81%)

external stimulus factors, the sensitivity of explosives could be sorted into impact sensitivity, friction sensitivity, and electrostatic spark sensitivity. Among them, impact sensitivity is studied frequently in experiment and theory. Since it was discovered that different crystal orientations of pentaerythritol tetranitrate (PETN) correspond to different impact sensitivity,[26] people began to focus on investigating anisotropic impact sensitivity using theoretical simulations.[25,27−29] Theoretical studies have shown that starting from the surface structure was a very effective method to study the anisotropy of impact sensitivity.[30,31]

The anisotropy of impact sensitivity is relevant to the thermodynamics and chemical reactions of explosives, which is essential to understand the reaction/explosion mechanism.[26,32,33] However, there has not been any report on anisotropic impact sensitivity of DAP-7 since it was synthesized. The goal of this study was to explore anisotropic impact sensitivity of DAP-7 based on density functional theory. The (100), (010), (011), (101), and (111) surfaces were studied from three aspects of electronic properties, surface energy, and hydrogen bonding in this work. Moreover, the corresponding properties of bulk crystal for DAP-7 were also investigated to form a comparison with the surface structures. This research could provide important theoretical supports for designing and developing newly energetic materials.

2. COMPUTATIONAL METHODS

All calculations in this paper were performed by using the Vienna Ab initio Simulation Package (VASP) code[34,35] in the framework of density functional theory (DFT). The projector augmented wave (PAW) method was used to describe interaction between the core and valence electrons.[36] Here, the model starting structure adopted the experimental structure of DAP-7 crystallized in a monoclinic lattice with $P2_1/m$ space group.[18] The unit cell of DAP-7 featured a hexagonal perovskite-type structure with the formula ABX_3, where A-site cation was H_2dabco^{2+}, B-site cation was $NH_2NH_3^+$, and X-site anion was ClO_4^-. The unit cell and ions structure of DAP-7 were displayed in Figure 1. The H($1s^1$), C($2s^22p^2$), N($2s^22p^3$), O($2s^22p^6$), and Cl($3s^23p^5$) were considered as the valence electrons.

First of all, the experimental crystal structure of DAP-7 performed full geometry optimizations which allow lattice parameters and atomic positions to be fully relaxed. The cutoff energy of plane waves was set to 450 eV. Gamma-centered Monkhorst−Pack k-point mesh of 3 × 4 × 3 was used for sampling the Brillouin zone in geometry optimization. The convergence criteria of energy and force was less than 10^{-5} eV and 0.03 eV/Å, respectively. In the case of hybrid perovskite materials, more accurate results could be obtained by considering the van der Waals (vdW) correction.[37] In terms of exchange correlation function, there were four functions tested to choose a more appropriate method in geometry optimization, including the Perdew, Burke, and Ernzerh of (PBE) functional,[38] the PBE functional revised for solids (PBEsol),[39] PBEsol plus the addition of Grimme's D3 dispersion correction (PBEsol+D3),[40] and the PBE functional plus the addition of D3 (PBE+D3).[41] The results are shown in Table 1. After that, they were cut along the (100), (010), (011), (101), and (111) crystal plane of the geometry-optimized crystal structure of DAP-7 and periodic conditions were applied to these surface models. The vacuum layer was set to 15 Å along the *Z*-direction, which was thick enough to avoid any interaction between the surfaces. To that end, the periodic surface models containing the (100), (010), (011), (101), and (111) surfaces could be obtained.

During the geometry optimizations of surface models, the cell parameters were fixed and only the atomic coordinates were optimized. Except for the K-point settings, the other parameters for geometry optimization, electronic properties, and surface energy calculations in the surface models were the same as those for the bulk crystal. The K points were set as Gamma-centered Monkhorst−Pack k-point mesh of 4 × 3 × 1, 3 × 3 × 1, 3 × 3 × 1, 3 × 4 × 1, and 3 × 3 × 1 during the

https://doi.org/10.1021/acsomega.2c00878
ACS Omega 2022, 7, 17185−17191

geometry optimization of the surface models of (100), (010), (011), (101), and (111), respectively.

3. RESULTS AND DISCUSSION

3.1. Crystal Structures and Surface Structures. The unit cell parameters of DAP-7 by experiment and DFT relaxed are tabulated in Table 1. It was found that the optimized structure by PBE+D3 was in good accordance with the experimental structure, whereas the PBE seemed to overestimate the lattice constants more drastically due to ignoring the van der Waals (vdW) correction. The errors of the lattice constants obtained by the methods of PBEsol and PBEsol+D3 were generally smaller than that of PBE but still larger than that of PBE+D3. Overall, the PBE+D3 functional was chosen as the optimal exchange correlation function in this paper. The unit cell structure optimized by PBE+D3 was used as the optimal structure. The optimized surface structures by PBE +D3 including (100), (010), (011), (101), and (111) were shown in Figure 2.

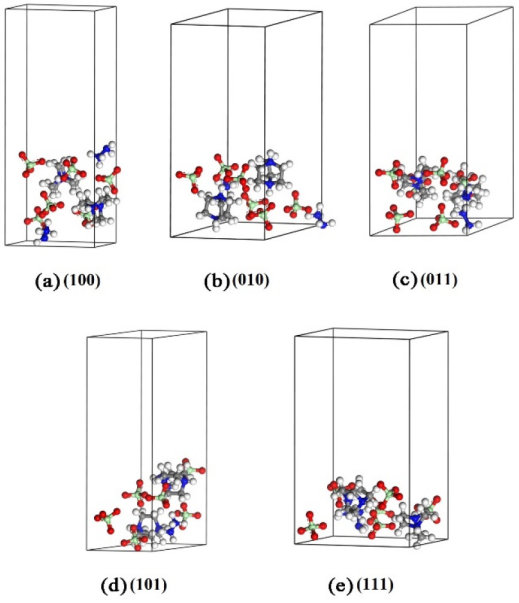

Figure 2. Different surface structures of DAP-7.

3.2. Electronic Structure. Band gap, the energy difference between the highest occupied molecular orbital (HOMO) and lowest unoccupied molecular orbital (LUMO), is an important parameter to characterize the electronic structure of crystals.[42] In the field of energetic materials, the band gap was closely related to the impact sensitivity, which was reflected in the fact that the initiation of energetic materials was accompanied by rupture of chemical bonds requiring population of antibonding state. Therefore, the electronic excitation generally resulted in a weakening of chemical bonds. Hence, the smaller the band gap was, the easier the electronic was to reach antibonding orbital, and the easier the chemical bond was to break.[43,44] According to the first-principles band gap criterion, a smaller band gap corresponds to a higher impact sensitivity for the energetic crystal with similar structure or thermal decomposition mechanism.[45−47] The first-principles band gap criterion has been widely used to predict impact sensitivity of various energetic compounds.[46−49]

To investigate the influence of surfaces on impact sensitivity of DAP-7, the band gap of bulk crystal and (100), (010), (011), (101), and (111) surfaces were calculated, and the results are given in Table 2. The sequence of band gap in

Table 2. Calculated Band Gap of Different Surfaces for DAP-7

contents	bulk	(100)	(010)	(011)	(101)	(111)
band gap (eV)	5.069	4.976	4.225	4.560	3.878	4.934

surface structures were (101) < (010) < (011) < (111) < (100), where the band gap value of the (100) surface was the largest and the band gap of the (101) surface was the smallest among these surfaces. The difference of band gap in surface structures of DAP-7 suggested that the impact sensitivities exhibit distinct anisotropic characteristics. According to the first-principles band gap criterion, it can be predicted that the impact sensitivities of surfaces in descending order were (101) > (010) > (011) > (111) > (100). The results showed that the (100) surface has the lowest impact sensitivity, whereas the (101) surface has the highest impact sensitivity. In addition, we found that the band gap values of these surfaces were smaller than that of the bulk crystal, suggesting that these surface structures show higher impact sensitivity than bulk crystal. This may result from the fact that the energetic molecules on the exposed surface show higher activities due to the reduced activation barriers.[50]

Electronic structure was an intrinsic factor that was critical in determining the impact sensitivities and chemical reactions of energetic materials. For the purpose of seeking more information about the impact sensitivity anisotropy from the electronic structure, the total density of states (TDOS) of bulk crystal and each surface of DAP-7 were investigated in this work, as depicted in Figure 3. Compared to the bulk crystal,

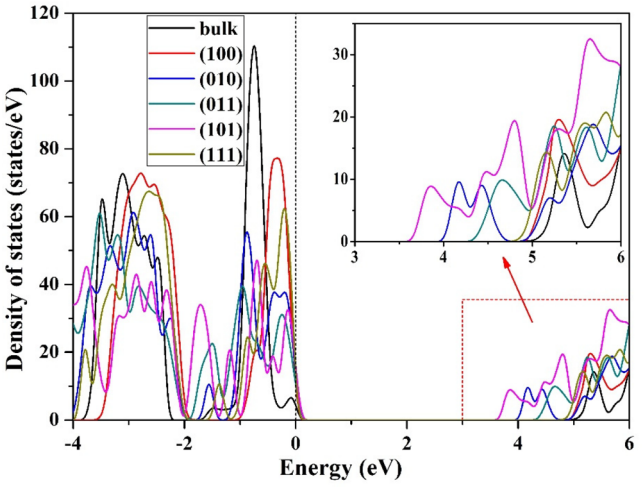

Figure 3. DOS for bulk crystal and different surfaces of DAP-7.

the TDOS of these surfaces migrated toward the lower energy region. The conduction bands of different surface structures were arranged from the low-energy region to the high-energy region as (101), (010), (011), (111), and (100) respectively. Observing the band gaps of the five surface structures mentioned above, it could be demonstrated that the more the conduction bands of the TDOS migrate to the lower energy region, the smaller the band gap is. By taking into

https://doi.org/10.1021/acsomega.2c00878
ACS Omega 2022, 7, 17185−17191

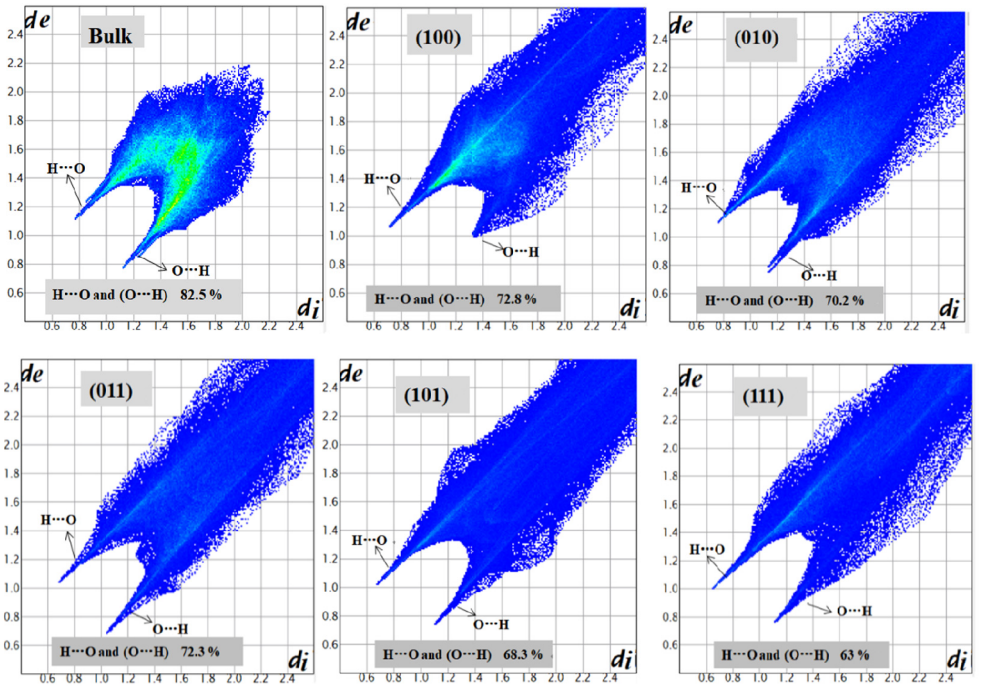

Figure 4. Fingerprint plots for bulk crystal and different surface structures of DAP-7.

account the relationship between the impact sensitivity and band gap, it was presumed that the more the conduction bands of the TDOS move toward lower energy, the more sensitive the surface is.

3.3. Surface Energy. The formation of surfaces could change the periodic potential field of the material, which may affect the anisotropic impact sensitivity.[30] Here, the surface energy of different surfaces was calculated and then compared with the impact sensitivity quantified by the band gap to study the relationship between the surface energy and impact sensitivity.

The surface energy can be applied to evaluate the stability of each kind of low index surfaces,[51] and it can be calculated by the following equation[52−55]

$$E_{surface} = \frac{E_{total}(n) - NE_{bulk}}{2A} \quad (1)$$

where $E_{surface}$ indicates the surface energy, E_{total} is the total energy of the surface model, E_{bulk} refers to the total energy of unit cell of DAP-7, A is the surface area of the surface, and N is the number of surface layers. The calculation results of surface energies in (100), (010), (011), (101), and (111) surfaces were 0.0482, 0.0808, 0.0678, 0.1437, and 0.0716 J/m^2, respectively. The sequence of surface energy of five surface structures in descending order was as follows: (101) > (010) > (111) > (011) > (100). Additionally, it could be found that the sequence of the surface energy was broadly consistent with the sequence of the impact sensitivity discussed in the previous section. Therefore, we presumed that the greater surface energy is, the more sensitive the surface would be, because increasing surface energy could result in the more active molecules favorable to the decomposition and explosion of explosives.

3.4. Hydrogen Bond. There exists a large number of H···O (or O···H) hydrogen bonding interactions in the crystal of DAP-7, and these hydrogen bonding interactions facilitated the face-sharing $B(ClO_4)_6$ octahedrons to be connected thus forming a hexagonal packing structure.[18] Hence, hydrogen bonding played a predominant role in the formation and stabilities of DAP-7.

It is well-known that hydrogen bonding was an important factor affecting the structural stability, thermodynamic properties, and molecular packing of energetic compounds.[56,57] The content of hydrogen bond could affect the binding energy between molecules. The more hydrogen bond content there is, the more impact energy is required by explosives to break the hydrogen bond net.[58] Therefore, the higher the hydrogen bond content is, the lower the impact sensitivity is.[57−59] Two-dimensional fingerprint plots could display the type and proportion of intermolecular interactions, providing important information for predicting the impact sensitivity of energetic materials.[48,60−62]

Figure 4 displays the fingerprint plots of bulk crystal and five surface structures. The percentage of O···H (H···O) interactions in the bulk crystal was higher than that of all surface structures, and the reason was that the existence of a vacuum layer in surfaces could weaken the intermolecular interactions. The percentages of O···H (H···O) in (100), (010), (011), (101), and (111) surfaces were 72.8%, 70.2%, 72.3%, 68.3%, and 63.0%, respectively. According to the relationship between hydrogen bonding and structural stability, it could be inferred that the sequence of impact sensitivity corresponding to the five surface structures is (111) > (101) > (010) > (011) > (100). Additionally, we could find that the result in this part was roughly consistent with that in the preceding part.

4. CONCLUSIONS

Density functional theory has been performed to investigate the electronic properties, surface energy, and hydrogen bonding in different surface structures of DAP-7. The lattice constants of the optimized bulk crystal showed that the simulation results obtained by the PBE+D3 method were in

https://doi.org/10.1021/acsomega.2c00878
ACS Omega 2022, 7, 17185−17191

good agreement with the experimental results. The calculated band gap values of the surface structures demonstrated that the impact sensitivity of different surfaces showed significant anisotropy. Especially, the impact sensitivity of (100) surface was considered to be the lowest among all surfaces. An analysis of the total density of states further validated the anisotropic properties obtained from the band gap, which was reflected by the varying magnitudes of migration of the total density of states on different surfaces relative to that of the bulk crystal. Since the order of surface energy was roughly consistent with the sequence of impact sensitivity quantified by band gap, we speculated that a larger surface energy corresponded to a higher impact sensitivity. The two-dimensional fingerprint plots indicated that the contents of hydrogen bonds in different surface structures showed significant variability. The (100) surface contained the most hydrogen bonds so that its impact sensitivity was the lowest. To summarize, the research on electronic properties, surface energy, and hydrogen bonding suggested that the impact sensitivity of different surface structures presents obvious anisotropy and the impact sensitivity of (100) surface is the lowest among all surface structures.

AUTHOR INFORMATION

Corresponding Author

Jijun Xiao − *Molecules and Materials Computation Institute, School of Chemistry and Chemical Engineering, Nanjing University of Science and Technology, Nanjing 210094, P.R. China*; orcid.org/0000-0003-0054-7957; Email: xiao_jijun@njust.edu.cn

Authors

Qiaoli Li − *Molecules and Materials Computation Institute, School of Chemistry and Chemical Engineering, Nanjing University of Science and Technology, Nanjing 210094, P.R. China*

Shenshen Li − *Molecules and Materials Computation Institute, School of Chemistry and Chemical Engineering, Nanjing University of Science and Technology, Nanjing 210094, P.R. China*

Minghe Qu − *Molecules and Materials Computation Institute, School of Chemistry and Chemical Engineering, Nanjing University of Science and Technology, Nanjing 210094, P.R. China*

Complete contact information is available at: https://pubs.acs.org/10.1021/acsomega.2c00878

Notes

The authors declare no competing financial interest.

ACKNOWLEDGMENTS

This work was funded by the grant from the National Natural Science Foundation of China (Grant 11572160).

REFERENCES

(1) Gao, H. X.; Shreeve, J. n. M. Azole-based energetic salts. *Chem. Rev.* **2011**, *111* (11), 7377−7436.

(2) Agrawal, J. P. *High energy materials: propellants, explosives and pyrotechnics*; John Wiley & Sons, 2010.

(3) Agrawal, J. P. Some new high energy materials and their formulations for specialized applications. *Propell. Explos. Pyrot.* **2005**, *30* (5), 316−328.

(4) He, P.; Mei, H. Z.; Wu, L.; Yang, J. Q.; Zhang, J. G.; Cohen, A.; Gozin, M. Design of new bridge-ring energetic compounds obtained by Diels−Alder reactions of tetranitroethylene dienophile. *J. Phys. Chem. A* **2018**, *122* (12), 3320−3327.

(5) Tang, Y. X.; He, C. L.; Imler, G. H.; Parrish, D. A.; Shreeve, J. n. M. Aminonitro groups surrounding a fused pyrazolotriazine ring: a superior thermally stable and insensitive energetic material. *ACS Appl. Energy Mater.* **2019**, *2* (3), 2263−2267.

(6) Zhao, G.; He, C. L.; Yin, P.; Imler, G. H.; Parrish, D. A.; Shreeve, J. n. M. Efficient construction of energetic materials via nonmetallic catalytic carbon−carbon cleavage/oxime-release-coupling reactions. *J. Am. Chem. Soc.* **2018**, *140* (10), 3560−3563.

(7) Snyder, C. J.; Wells, L. A.; Chavez, D. E.; Imler, G. H.; Parrish, D. A. Polycyclic N-oxides: high performing, low sensitivity energetic materials. *Chem. Commun.* **2019**, *55* (17), 2461−2464.

(8) Xue, M. N.; Zhou, H.; Xu, Y.; Mei, J.; Yang, L.; Ye, C.; Zhang, J.; Wang, H. High-performance ultraviolet-visible tunable perovskite photodetector based on solar cell structure. *Science China Materials* **2017**, *60* (5), 407−414.

(9) Vakharia, V.; Castelli, I. E.; Bhavsar, K.; Solanki, A. Bandgap prediction of metal halide perovskites using regression machine learning models. *Phys. Lett. A* **2022**, *422*, 127800.

(10) Liu, G. C.; Liu, Z. H.; Wang, L.; Xie, X. Y. An organic-inorganic hybrid hole transport bilayer for improving the performance of perovskite solar cells. *Chem. Phys.* **2021**, *542*, 111061.

(11) Lang, L.; Yang, J. H.; Liu, H. R.; Xiang, H. J.; Gong, X. G. First-principles study on the electronic and optical properties of cubic ABX3 halide perovskites. *Phys. Lett. A* **2014**, *378* (3), 290−293.

(12) Ye, H. Y.; Tang, Y. Y.; Li, P. F.; Liao, W. Q.; Gao, J. X.; Hua, X. N.; Cai, H.; Shi, P. P.; You, Y. M.; Xiong, R. S. Metal-free three-dimensional perovskite ferroelectrics. *Science* **2018**, *361* (6398), 151−155.

(13) Liao, W. Q.; Zhao, D. W.; Tang, Y. Y.; Zhang, Y.; Li, P. F.; Shi, P. P.; Chen, X. G.; You, Y. M.; Xiong, R. G. A molecular perovskite solid solution with piezoelectricity stronger than lead zirconate titanate. *Science* **2019**, *363* (6432), 1206−1210.

(14) Xing, G. C.; Mathews, N.; Lim, S. S.; Yantara, N.; Liu, X. F.; Sabba, D.; Grätzel, M.; Mhaisalkar, S.; Sum, T. C. Low-temperature solution-processed wavelength-tunable perovskites for lasing. *Nat. Mater.* **2014**, *13* (5), 476−480.

(15) Qi, X.; Zhang, Y. P.; Ou, Q. D.; Ha, S. T.; Qiu, C. W.; Zhang, H.; Cheng, Y. B.; Xiong, Q. H.; Bao, Q. L. Photonics and optoelectronics of 2D metal-halide perovskites. *Small* **2018**, *14* (31), 1800682.

(16) Chen, S. L.; Shang, Y.; He, C. T.; Sun, L. Y.; Ye, Z. M.; Zhang, W. X.; Chen, X. M. Optimizing the oxygen balance by changing the A-site cations in molecular perovskite high-energetic materials. *CrystEngComm* **2018**, *20* (46), 7458−7463.

(17) Chen, S. L.; Shang, Y.; He, C. T.; Sun, L. Y.; Ye, Z. M.; Zhang, W. X.; Chen, X. M. Optimizing the oxygen balance by changing the A-site cations in molecular perovskite high-energetic materials. *CrystEngComm* **2018**, *20* (46), 7458−7463.

(18) Shang, Y.; Yu, Z. H.; Huang, R. K.; Chen, S. L.; Liu, D. X.; Chen, X. X.; Zhang, W. X.; Chen, X. M. Metal-free hexagonal perovskite high-energetic materials with NH3OH+/NH2NH3+ as B-site cations. *Engineering* **2020**, *6* (9), 1013−1018.

(19) Liu, Y.; Hu, L. S.; Gong, S. D.; Guang, C. Y.; Li, L. Q.; Hu, S. Q.; Deng, P. Study of ammonium perchlorate-based molecular perovskite $(H_2dabco)[NH_4(ClO_4)_3]$/graphene energetic composite with insensitive performance. *Chem. Technol.* **2020**, *17* (3), 451−469.

(20) Deng, P.; Ren, H.; Jiao, Q. J. Enhanced the combustion performances of ammonium perchlorate-based energetic molecular perovskite using functionalized graphene. *Vacuum* **2019**, *169*, 108882.

(21) Li, X. X.; Hu, S. Q.; Cao, X.; Hu, L. S.; Deng, P.; Xie, Z. B. Ammonium perchlorate-based molecular perovskite energetic materials: preparation, characterization, and thermal catalysis performance with MoS2. *Journal of Energetic Materials* **2020**, *38* (2), 162−169.

(22) Han, K.; Zhang, X.; Deng, P.; Jiao, Q.; Chu, E. Study of the thermal catalysis decomposition of ammonium perchlorate-based

molecular perovskite with titanium carbide MXene. *Vacuum* **2020**, *180*, 109572.
(23) Deng, P.; Wang, H.; Yang, X.; Ren, H.; Jiao, Q. Thermal decomposition and combustion performance of high-energy ammonium perchlorate-based molecular perovskite. *J. Alloy. Compd.* **2020**, *827*, 154257.
(24) Zhou, J.; Ding, L.; Zhao, F. Q.; Wang, B. Z.; Zhang, J. L. Thermal studies of novel molecular perovskite energetic material (C6H14N2)[NH4 (ClO4) 3]. *Chin. Chem. Lett.* **2020**, *31* (2), 554−558.
(25) Abraham, B. M. High pressure structural behaviour of 5,5′-bitetrazole-1,1′-diolate based energetic materials: a comparative study from first principles calculations. *RSC Adv.* **2020**, *10* (42), 24867−24876.
(26) Dick, J. J. Effect of crystal orientation on shock initiation sensitivity of pentaerythritol tetranitrate explosive. *Appl. Phys. Lett.* **1984**, *44* (9), 859−861.
(27) Zhou, T. T.; Lou, J. F.; Song, H. J.; Huang, F. L. Anisotropic shock sensitivity in a single crystal δ-cyclotetramethylene tetranitramine: a reactive molecular dynamics study. *Phys. Chem. Chem. Phys.* **2015**, *17* (12), 7924−7935.
(28) Ge, N.; Wei, Y. K.; Song, Z. F.; Chen, X. R.; Ji, G. F.; Zhao, F.; Wei, D. Q. Anisotropic responses and initial decomposition of condensed-phase β-HMX under shock loadings via molecular dynamics simulations in conjunction with multiscale shock technique. *J. Phys. Chem. B* **2014**, *118* (29), 8691−8699.
(29) Zhou, T.; Zybin, S. V.; Liu, Y.; Huang, F.; Goddard, W. A., III Anisotropic shock sensitivity for β-octahydro-1, 3, 5, 7-tetranitro-1, 3, 5, 7-tetrazocine energetic material under compressive-shear loading from ReaxFF-lg reactive dynamics simulations. *J. Appl. Phys.* **2012**, *111* (12), 124904.
(30) Zhong, M.; Qin, H.; Liu, Q. J.; Jiao, Z.; Zhao, F.; Shang, H. L.; Liu, F. S.; Liu, Z. T. Influences of different surfaces on anisotropic impact sensitivity of hexahydro-1, 3, 5-trinitro-1, 3, 5-triazine. *Vacuum* **2017**, *139*, 117−121.
(31) Zhong, M.; Qin, H.; Liu, Q. J.; Jiang, C. L.; Zhao, F.; Shang, H. L.; Liu, F. S.; Tang, B. A systematic study of the surface structures and energetics of CH_3NO_2 surfaces by first-principles calculations. *J. Mol. Model* **2019**, *25* (6), 1−8.
(32) Dick, J. J.; Hooks, D. E.; Menikoff, R.; Martinez, A. R. Elastic−plastic wave profiles in cyclotetramethylene tetranitramine crystals. *J. Appl. Phys.* **2004**, *96* (1), 374−379.
(33) Dick, J. J.; Mulford, R. N.; Spencer, W. J.; Pettit, D. R.; Garcia, E.; Shaw, D. C. Shock response of pentaerythritol tetranitrate single crystals. *J. Appl. Phys.* **1991**, *70* (7), 3572−3587.
(34) Kohn, W.; Sham, L. J. Self-consistent equations including exchange and correlation effects. *Phys. Rev.* **1965**, *140* (4A), A1133.
(35) Kresse, G.; Furthmüller, J. Efficiency of ab-initio total energy calculations for metals and semiconductors using a plane-wave basis set. *Comput. Mater. Sci.* **1996**, *6* (1), 15−50.
(36) Kresse, G.; Joubert, D. From ultrasoft pseudopotentials to the projector augmented-wave method. *Phys. Rev. B* **1999**, *59* (3), 1758.
(37) Tang, G.; Yang, C.; Stroppa, A.; Fang, D. N.; Hong, J. W. Revealing the role of thiocyanate anion in layered hybrid halide perovskite $(CH_3NH_3)_2Pb(SCN)_2I_2$. *J. Chem. Phys.* **2017**, *146* (22), 224702.
(38) Perdew, J. P.; Burke, K.; Ernzerhof, M. Generalized gradient approximation made simple. *Phys. Rev. Lett.* **1996**, *77* (18), 3865.
(39) Perdew, J. P.; Ruzsinszky, A.; Csonka, G. I.; Vydrov, O. A.; Scuseria, G. E.; Constantin, L. A.; Zhou, X. L.; Burke, K. Restoring the density-gradient expansion for exchange in solids and surfaces. *Phys. Rev. Lett.* **2008**, *100* (13), 136406.
(40) Grimme, S. Accurate description of van der Waals complexes by density functional theory including empirical corrections. *J. Comput. Chem.* **2004**, *25* (12), 1463−1473.
(41) Ganose, A. M.; Savory, C. N.; Scanlon, D. O. $(CH_3NH_3)_2Pb(SCN)_2I_2$: A more stable structural motif for hybrid halide photovoltaics? *J. Phys. Chem. Lett.* **2015**, *6* (22), 4594−4598.
(42) Zhu, W. H.; Xiao, H. M. First-principles study of electronic, absorption, and thermodynamic properties of crystalline styphnic acid and its metal salts. *J. Phys. Chem. B* **2009**, *113* (30), 10315−10321.
(43) Michalchuk, A. A.; Rudić, S.; Pulham, C. R.; Morrison, C. A. Vibrationally induced metallisation of the energetic azide α-NaN_3. *Phys. Chem. Chem. Phys.* **2018**, *20* (46), 29061−29069.
(44) Michalchuk, A. A.; Trestman, M.; Rudić, S.; Portius, P.; Fincham, P. T.; Pulham, C. R.; Morrison, C. A. Predicting the reactivity of energetic materials: an ab initio multi-phonon approach. *J. Mater. Chem. A* **2019**, *7* (33), 19539−19553.
(45) Zhu, W. H.; Xiao, H. M. First-principles band gap criterion for impact sensitivity of energetic crystals: a review. *Struct. Chem.* **2010**, *21* (3), 657−665.
(46) Wu, Q.; Zhu, W. H.; Xiao, H. M. Structural transformations and absorption properties of crystalline 7-amino-6-nitrobenzodifuroxan under high pressures. *J. Phys. Chem. C* **2013**, *117* (33), 16830−16839.
(47) Pallewela, G. N.; Bettens, R. P. A. Theoretical investigation of impact sensitivity of nitrogen rich energetic salts. *Comput. Theor. Chem.* **2021**, *1201*, 113267.
(48) Wu, Q.; Li, M. Q.; Hu, Q. N.; Zhang, Z. W.; Zhu, W. H. First-principle study and Hirshfeld surface analysis on the effect of H_2O, NH_3 and H_2S on structural, electronic, elastic, optical and thermodynamic properties of a novel high-energy crystal 2, 4, 6-triamino-5-nitropyrimidine-1, 3-dioxide. *J. Mater. Sci.* **2020**, *55* (1), 237−249.
(49) Zhu, W. H.; Xiao, J. J.; Ji, G. F.; Zhao, F.; Xiao, H. M. First-principles study of the four polymorphs of crystalline octahydro-1, 3, 5, 7-tetranitro-1, 3, 5, 7-tetrazocine. *J. Phys. Chem. B* **2007**, *111* (44), 12715−12722.
(50) Sharia, O.; Kuklja, M. M. Surface-enhanced decomposition kinetics of molecular materials illustrated with cyclotetramethylene-tetranitramine. *J. Phys. Chem. C* **2012**, *116* (20), 11077−11081.
(51) Zhou, Y.; Xiong, H. H.; Yin, Y. H.; Zhong, S. W. First principles study of surface properties and oxygen adsorption on the surface of Al_3Ti intermetallic alloys. *RSC Adv.* **2019**, *9* (4), 1752−1758.
(52) Sharia, O.; Tsyshevsky, R.; Kuklja, M. M. Surface-accelerated decomposition of δ-HMX. *J. Phys. Chem. Lett.* **2013**, *4* (5), 730−734.
(53) Gurdal, Y.; Luber, S.; Hutter, J.; Iannuzzi, M. Non-innocent adsorption of Co-pyrphyrin on rutile (110). *Phys. Chem. Chem. Phys.* **2015**, *17* (35), 22846−22854.
(54) Creazzo, F.; Luber, S. Explicit solvent effects on (1 1 0) ruthenium oxide surface wettability: Structural, electronic and mechanical properties of rutile RuO_2 by means of spin-polarized DFT-MD. *Appl. Surf. Sci.* **2021**, *570*, 150993.
(55) Mou, J.; Gao, Y.; Wang, J.; Ma, J.; Ren, H. Hydrogen evolution reaction activity related to the facet-dependent electrocatalytic performance of NiCoP from first principles. *RSC Adv.* **2019**, *9* (21), 11755−11761.
(56) Spackman, M. A.; Jayatilaka, D. Hirshfeld surface analysis. *CrystEngComm* **2009**, *11* (1), 19−32.
(57) Feng, S. B.; Yin, P.; He, C. L.; Pang, S. P.; Jean'ne, M. S. Tunable Dimroth rearrangement of versatile 1, 2, 3-triazoles towards high-performance energetic materials. *J. Mater. Chem. A* **2021**, *9* (20), 12291−12298.
(58) Tan, B. S.; Long, X. P.; Peng, R. F.; Li, H. B.; Jin, B.; Chu, S. J.; Dong, H. S. Two important factors influencing shock sensitivity of nitro compounds: Bond dissociation energy of X−NO_2 (X= C, N, O) and Mulliken charges of nitro group. *J. Hazard. Mater.* **2010**, *183* (1−3), 908−912.
(59) Zhang, J. H.; Zhang, Q. H.; Vo, T. T.; Parrish, D. A.; Shreeve, J. n. M. Energetic salts with π-stacking and hydrogen-bonding interactions lead the way to future energetic materials. *J. Am. Chem. Soc.* **2015**, *137* (4), 1697−1704.
(60) Zhang, W. Q.; Zhang, J. H.; Deng, M. C.; Qi, X. J.; Nie, F. D.; Zhang, Q. H. A promising high-energy-density material. *Nat. Commun.* **2017**, *8*, 181.

https://doi.org/10.1021/acsomega.2c00878
ACS Omega 2022, 7, 17185−17191

(61) Tian, B. B.; Xiong, Y.; Chen, L. Z.; Zhang, C. Y. Relationship between the crystal packing and impact sensitivity of energetic materials. *CrystEngComm* **2018**, *20* (6), 837−848.
(62) Ma, Y.; Meng, L. Y.; Li, H. Z.; Zhang, C. Y. Enhancing intermolecular interactions and their anisotropy to build low-impact-sensitivity energetic crystals. *CrystEngComm* **2017**, *19* (23), 3145−3155.

https://doi.org/10.1021/acsomega.2c00878
ACS Omega 2022, 7, 17185−17191